



Assessment of Overmodulation Strategies for AC Drives Considering Harmonics Content and Switching Losses

Ahmed Fathy Abouzeid 
Dept. of Electrical Engineering
University of Oviedo
Gijón, Spain
abouzeidahmed@uniovi.es

Juan Manuel Guerrero 
Dept. of Electrical Engineering
University of Oviedo
Gijón, Spain
guerrero@uniovi.es

Aitor Endemaño
Traction systems
Ingeteam Power Technology
Zamudio, Spain
aitor.endemano@ingeteam.com

Iker Muniategui
Traction systems
Ingeteam Power Technology
Zamudio, Spain
iker.muniategui@ingeteam.com

David Ortega
Traction systems
Ingeteam Power Technology
Zamudio, Spain
David.Ortega@ingeteam.com

Fernando Briz 
Dept. of Electrical Engineering
University of Oviedo
Gijón, Spain
fbriz@uniovi.es

Abstract—This paper performs a comparative analysis of overmodulation methods for AC electric drives. Criteria for the analysis considers three aspects: output vs. commanded modulation index (i.e., linearity); harmonic content; and the number of commutations (i.e., switching losses). The analysis focuses on existing methods reported in the literature. Improvements for the existing methods will be proposed as a result of the analysis. The analysis is experimentally validated on a three-phase three-level Neutral-Point-Clamped (NPC) inverter.

I. INTRODUCTION

Overmodulation is used in electric drives to increase the fundamental output voltage of the inverter. This has two beneficial effects: 1) an increase of the fundamental output voltage allows to get more torque at high speed, and consequently more power; 2) the number of commutations, and consequently, the switching losses in the inverter are reduced [1]. Unfortunately, this is at the price of an increase of the distortion of the currents creating torque harmonics with the subsequent effects as noise, vibration, additional losses in the machine, etc [2]. Many efforts have been devoted to improving drive performance in overmodulation [3]–[9]. However, the analyses reported in the literature primarily focuses on voltage utilization and harmonic content, the effect on switching losses being normally ignored. This paper presents a comparative analysis of overmodulation methods for AC electric drives using three criteria: output vs. commanded modulation index (i.e. linearity); harmonic content; and number of commutations (i.e. switching losses). Thus, the analysis will primarily focus on existing methods reported in the literature, followed by a generalized form for improving some of these methods will be also addressed. Though the methods discussed in this paper can be applied to any electric drive, they will be of especial relevance in high power applications in which machine and/or

power converter need to operate close to their thermal limits, as often occurs in railway traction drives.

II. VOLTAGE SYNTHESIS SUMMARY OF OVERMODULATION STRATEGIES

The modulation index (M_i) of a three-phase inverter is given by (1), where V is the peak value of the phase voltage fundamental component and V_{dc} is the inverter dc input voltage. Modulation methods as Space-Vector Modulation (SVM) or sine-triangle Pulse-Width Modulation (PWM) with triplen harmonic injection allow linear operation of the inverter (i.e. $M_i = M_i^*$) up to $M_i = 0.907$, $M_i = 1$ being achieved with six-step modulation.

$$M_i = \frac{V}{\frac{2}{\pi}V_{dc}} \quad (1)$$

In the overmodulation range ($0.907 \leq M_i \leq 1$), the voltage waveform is distorted, which results in odd harmonics. In addition, the relationship between commanded and actual modulation index, M_i^* and M_i , becomes non-linear. Several overmodulation methods that have been reported in the literature will be summarized following (see Fig. 2), and their performance will be discussed in Section IV:

A. Minimum-Phase Error (MPE), V_{s1}^*

In this strategy, when the reference voltage vector V_s^* is outside the hexagon, the applied voltage is obtained as the intersection between the voltage command and the hexagon boundary [10]. The results for this method has been omitted from the paper as it requires infinity gain to reach six-step operation.

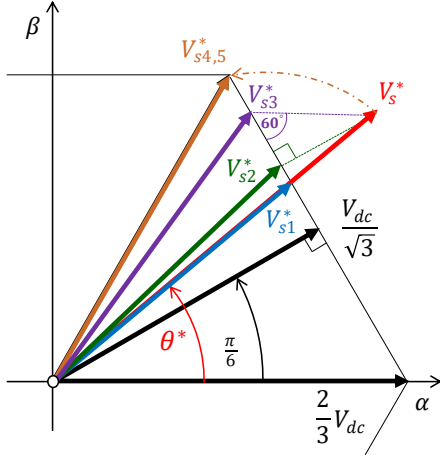


Fig. 1: Space-vector representation of the modified voltage vector vs. the reference voltage vector for overmodulation.

B. Minimum-Distance/Magnitude Error (MDE), V_{s2}^*

When the reference voltage vector is outside the hexagon, the output voltage is obtained as the projection of the voltage command orthogonal to the hexagon boundary (see Fig. 2a) [10].

C. Switching-state (60°), V_{s3}^*

The output voltage vector is modified to a point in which the vector difference between the reference and the output voltage vector makes a 60° lagging/leading with the hexagon boundary on the first/second half of each hexagon sector respectively (see Fig. 2b) [10].

D. Single-mode, V_{s4}^*

When the reference vector exceeds the hexagon boundary, the output voltage vector is obtained by rotating the reference voltage, keeping its magnitude constant, until it touches the hexagon boundary (see Fig. 2c). With this method, six-step operation is reached when $V^* = \frac{2}{3}V_{dc}$ [11]. Due to holding the reference voltage vector at the intersection point, the phase angle of the reference vector is shifting to the next or the previous intersection point depending on its location in the sector. This results in a significant increase of harmonic components in the output voltage.

E. Dual-mode, V_{s5}^*

This method is intended to overcome the single-mode high harmonic content [12], [13]. Overmodulation is divided into two modes: a) Mode I ($0.907 < M_i \leq 0.952$): only the magnitude of the reference vector is changed while the phase angle is kept as its reference. If the reference vector is outside the hexagon boundary, the output vector is limited to the hexagon bounds. When the reference vector is inside the hexagon, the output vector magnitude is increased with an appropriate value to compensate for the difference in the reference vector during the operation outside the hexagon limit.

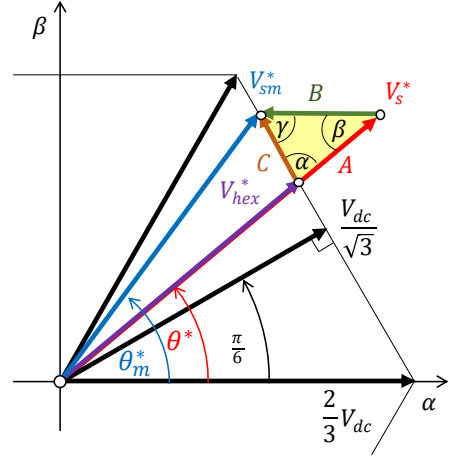


Fig. 3: Proposed generalized form overmodulation strategy: a) Reference voltage vector, V_s^* ; b) Modified reference voltage vector with an arbitrary angle γ , V_{sm}^* .

The modified vector magnitude is a function of the reference angle α_r . b) Mode II ($0.952 < M_i \leq 1$): both vector magnitude and phase angle are changed to ensure a smooth transition of the output voltage vector into square wave, i.e. six-step (see Fig. 2d). The output voltage vector is limited to the hexagon boundary while the output phase angle is modified according to a holding angle α_h which is gradually increased from zero to $\frac{\pi}{6}$ at six-step. For online implementation both the reference and the holding angles are linearized as a function of the modulation index [13].

III. GENERALIZED FORM OF SPACE-VECTOR PWM IN OVERMODULATION

From the previous discussion, it can be noticed that the Minimum-Phase Error, Minimum-Distance Error and Switching-State methods are based on similar principles, the only difference being the angle between the voltage vector being added to the original voltage command and the hexagon boundary (0° , 90° and 60° respectively), as seen in Fig. 1. This type of overmodulation can be generalized to any arbitrary angle γ as described following:

- 1) Assuming the reference voltage vector is located in the first sector. The reference vector magnitude limited to the hexagon boundary is calculated in (2), where θ^* is the angle of the reference voltage vector.

$$|V_{hex}^*| = \frac{V_{dc}}{\sqrt{3} \cos(\theta^* - \frac{\pi}{6})} \quad (2)$$

- 2) For a given angle γ the triangle ABC shown in Fig. 3 is formed, with the angles α and β being obtained as:

$$\alpha = \begin{cases} \theta^* + \frac{\pi}{3}, & \text{if } 0 \leq \theta^* \leq \frac{\pi}{6} \\ \pi - \theta^* - \frac{\pi}{3}, & \text{if } \frac{\pi}{6} < \theta^* \leq \frac{\pi}{3} \end{cases} \quad (3)$$

$$\beta = \pi - \alpha - \gamma. \quad (4)$$

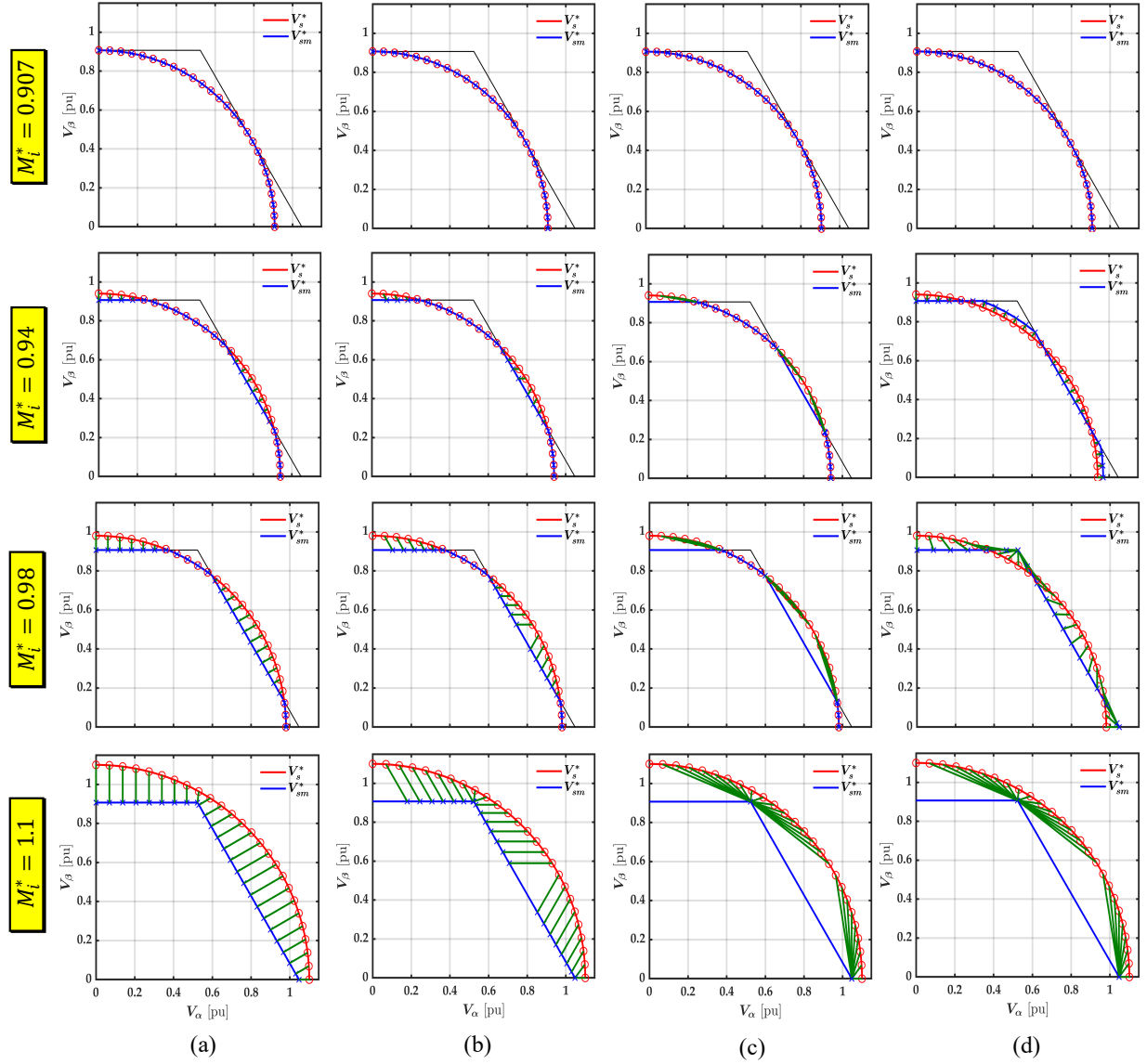


Fig. 2: Reference voltage vector synthesis using different overmodulation methods: (a) Minimum-Distance Error (90°); (b) Switching-State (60°); (c) Single-mode; (d) Dual-mode. Red: reference voltage vector. Blue: modified reference voltage vector. Green: difference between reference and modified voltage vectors.

3) The modified reference vector can be calculated as follows:

$$|A| = |V_s^*| - |V_{hex}^*| \quad (5)$$

$$|C| = |A| \frac{\sin(\beta)}{\sin(\gamma)} \quad (6)$$

$$\vec{V}_{sm}^* = \begin{cases} \vec{V}_{hex}^* + |C| e^{-j\frac{\pi}{3}}, & \text{if } 0 \leq \theta^* \leq \frac{\pi}{6} \\ \vec{V}_{hex}^* + |C| e^{j\frac{2\pi}{3}}, & \text{if } \frac{\pi}{6} < \theta^* \leq \frac{\pi}{3} \end{cases} \quad (7)$$

4) Finally, the modified reference voltage vector \vec{V}_{sm}^* is rotated for the remaining sectors.

IV. COMPARATIVE ANALYSIS OF OVERMODULATION STRATEGIES

This section compares the performance of the different overmodulation strategies. As already stated, three aspects will be considered: a) output to commanded modulation index (linearity); b) harmonic distortion; and c) number of commutations. The analysis will focus on strategies which can reach six-step operation; hence the Minimum-Phase Error (MPE) method is disregarded as it requires an infinite reference modulation index to reach six-step.

Fig. 4a shows the actual (M_i) vs. commanded (M_i^*) modulation index for the overmodulation methods stated in section II. It is seen that the Dual-mode strategy provides a nearly

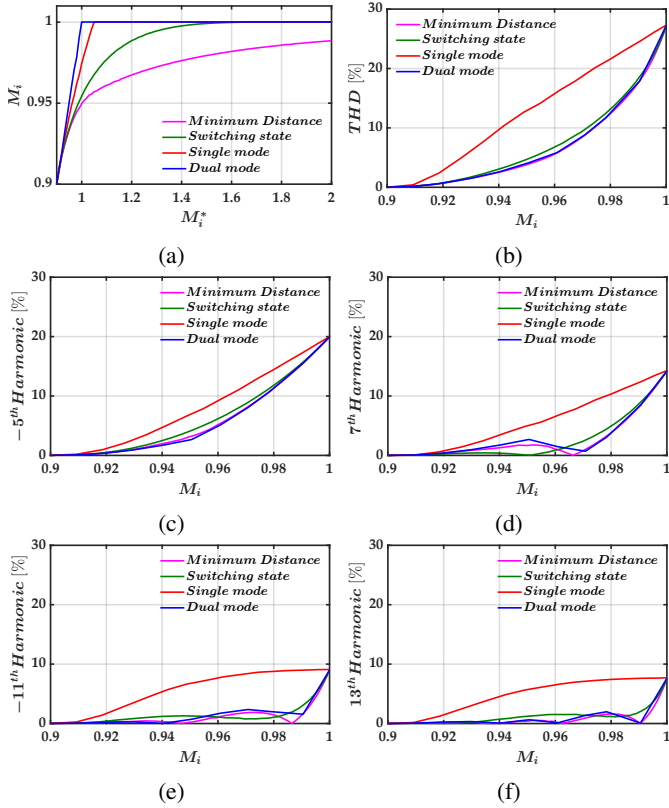


Fig. 4: Comparative analysis: a) M_i versus M_i^* ; b) THD, c) -5^{th} , d) 7^{th} , e) -11^{th} and f) 13^{th} harmonic components vs. M_i respectively.

linear relationship between the reference and the output voltage while the Minimum-Distance Error (MDE) one shows the worse behavior in this regard. The six-step operation is reached at a very high (in the range of thousands) value of the reference modulation index, therefore the reference modulation index in Fig. 4a is only showed up to the value of 2 for clear visualization and comparison with other methods. Switching-State strategy modifies the reference voltage vector to be 60° from the hexagon boundary. Six-step operation is achieved in this case for $M_i^* \cong 1.5$. Holding the reference voltage vector at the hexagon boundary to compensate for the interval being outside the hexagon (i.e. Single-mode), will fasten the achievability of the six-step operation to $M_i^* \cong 1.047$ [11].

To conclude this discussion, it is important to note that the non-linear relationship between the commanded and actual modulation index can potentially be compensated by pre-warping the commanded modulation index, either a look-up table or an analytical function can be used for this purpose.

The main concern using overmodulation are the low-order harmonics introduced in the output voltage waveform, which will be transferred to the currents and eventually to torque. Fig. 4b shows the Total Harmonic Distortion (THD) considering the -5^{th} , 7^{th} , -11^{th} and 13^{th} harmonic components. It is noted that the Single-mode method shows the worst behavior, while for the other methods subject of this analysis only minor

differences are observed. The individual harmonic distortion for the -5^{th} , 7^{th} , -11^{th} and 13^{th} components are shown in Fig. 4c-f respectively. It is seen that Minimum-Distance Error and Dual-mode have lower harmonic content for most of the overmodulation range. However, the Switching-State method has lower distortion in certain harmonic components for a specific modulation index range. For instance, the 7^{th} from $M_i^* = 0.9$ to $M_i^* = 0.95$ and the -11^{th} from $M_i^* = 0.958$ to $M_i^* = 0.98$, Switching-State method becomes superior for these ranges regarding to harmonic content.

Another important aspect which is often neglected in the literature are the switching losses, which are especially relevant for medium-voltage high-power drives. The number of commutations per quarter of cycle was obtained by means of simulation. This number is a function of the modulation index and the ratio between switching frequency and fundamental frequency, $(\frac{\omega_{sw}}{\omega_f})$. Fig. 5 shows the results for a ratio of 100 and 10 respectively. The Single-mode strategy shows the worst performance, while none of the other methods is superior (i.e., has less commutations) for all modulation indexes and switching to fundamental ratios.

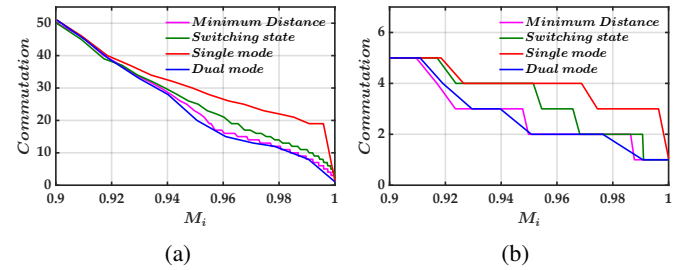


Fig. 5: Number of commutations per quarter cycle of the fundamental frequency, of the different overmodulation methods vs. M_i for a switching to fundamental frequency ratio: a) $\frac{\omega_{sw}}{\omega_f} = 100$; b) $\frac{\omega_{sw}}{\omega_f} = 10$.

The same analyses was repeated using the proposed general form discussed in section III. By comparing the results in Fig. 6 and Fig. 7, it can be concluded that the lower the angle, the higher the linearity, THD, and number of commutations. The maximum output voltage is found at 1.047 of the commanded modulation indexes, which is similar to the Single-mode method. But again, taking into consideration the individual low-order harmonic components, none of the angles provides the best solution over the whole overmodulation range.

Optimal overmodulation strategy can be achieved by combining at least two overmodulation methods as a function of modulation index. As the minimum number of commutations and minimum low-order harmonic distortion (especially -5^{th} & 7^{th}) are usually the requirements for traction drives, a combination of Switching-State and Dual-mode could provide the best performance over the whole overmodulation range.

V. EXPERIMENTAL VALIDATION

Fig. 8 shows the hardware setup of the test bench used for experimental verification. Control is implemented on a

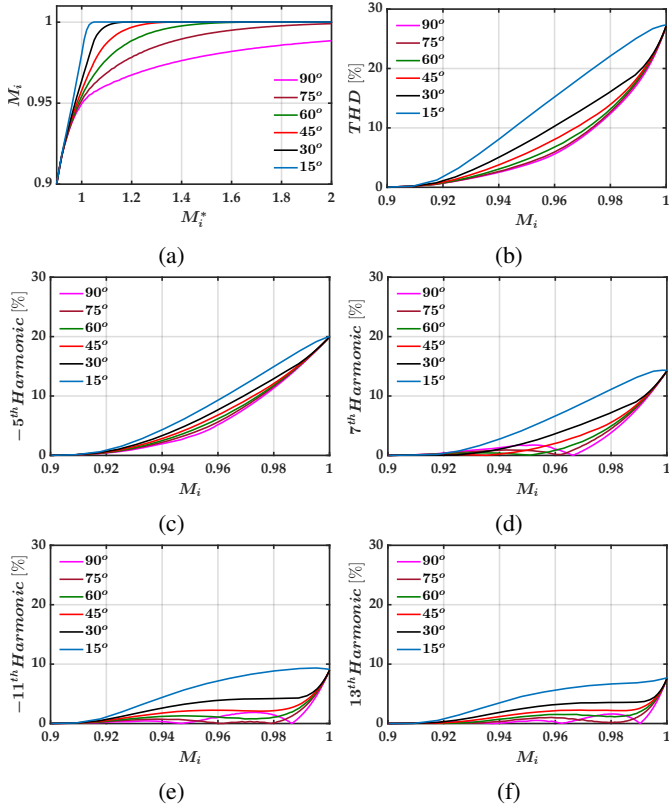


Fig. 6: Comparative analysis as a function of γ angle: a) M_i versus M_i^* ; b) THD, c) -5^{th} , d) 7^{th} , e) -11^{th} and f) 13^{th} harmonic components vs. M_i respectively.

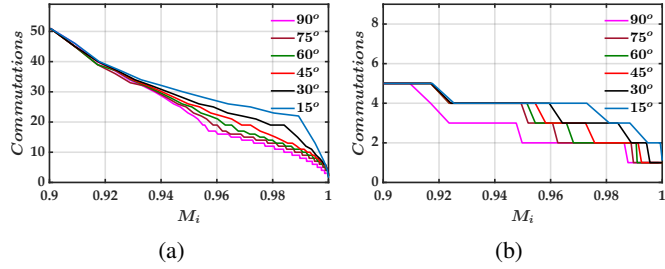


Fig. 7: Number of commutations per quarter cycle of the fundamental frequency, of the different overmodulation methods as a function of γ angle vs. M_i for a switching to fundamental frequency ratio: a) $\frac{\omega_{sw}}{\omega_f} = 100$; b) $\frac{\omega_{sw}}{\omega_f} = 10$.

TMS320F28335 DSP. A three-level 4 kV NPC three-phase inverter was used. For the experiments presented in this paper, the dc-link was limited to 600V. The switching and sampling frequencies are 1 kHz, a dead-time of 4 μ s is used.

The measured phase-a to dc mid-point voltages is shown in Fig. 9. It can be noticed that the switching pattern of Minimum-Distance Error and Switching-State methods are still far from six-step operation even at ($M_i^* = 1.1$). The transition from linear modulation to six-step is achieved in both Single-mode (see Fig. 9c) and Dual-mode (see Fig. 9d). However, Dual-mode reaches six-step faster with less number

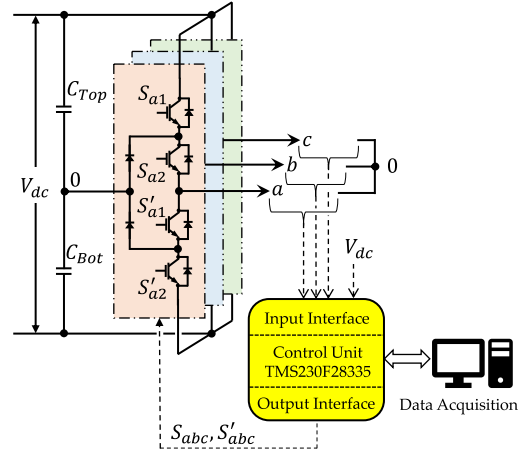


Fig. 8: Test bench for overmodulation strategies: a) Schematic representation of the laboratory setup; b) 4 kV/40A three-level NPC ELINSA inverter.

of commutations which confirms the simulation results in section IV (see Fig. 9c vs. Fig. 9d at $M_i^* = 0.94$ and $M_i^* = 0.98$).

Despite of the main aspects compared in this section, the dynamic performance plays an important role in selecting the appropriate overmodulation strategy for electric drives. Usually, overmodulation methods with larger gains are preferred for such applications which involves current regulators [14], [15]. Further investigation of the dynamic performance of overmodulation strategies and the transition from one method to another for optimal overmodulation is ongoing.

VI. CONCLUSIONS

In this paper, comparative analysis of four overmodulation strategies for electric drives reported in the literature is performed: Minimum-Distance Error (90°), Switching-State (60°), Single-mode, and Dual-mode. Furthermore, a generalized overmodulation method with an arbitrary angle γ is presented. Criteria considered for the analysis are: 1) linearity,

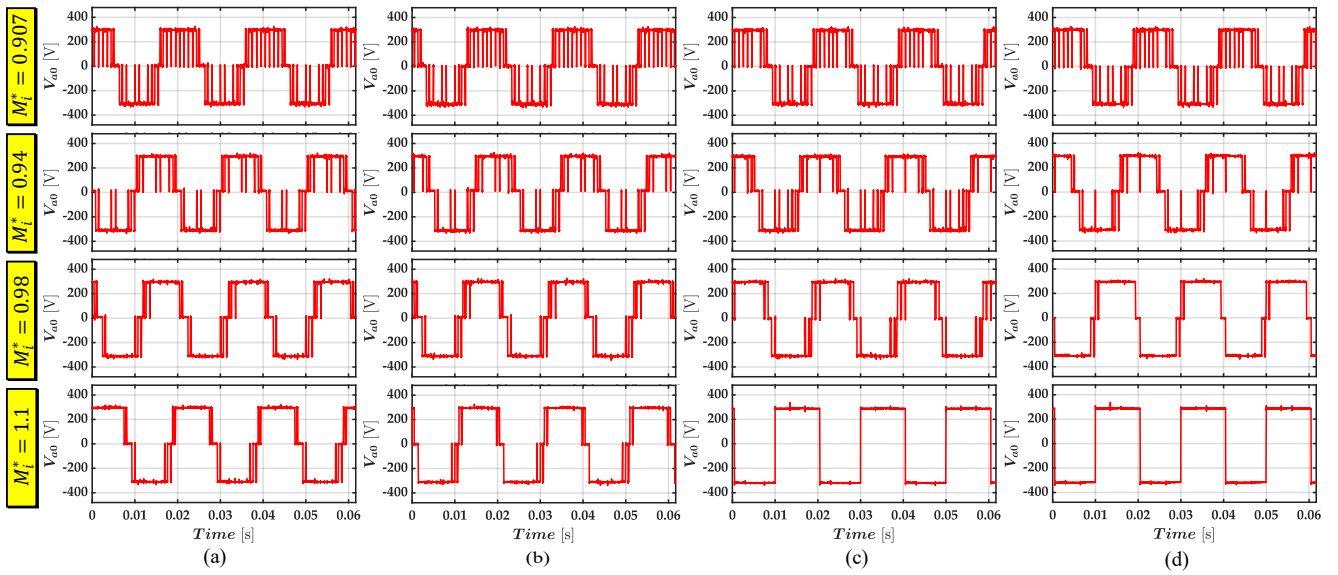


Fig. 9: Measured voltage of phase a to dc mid-point of three-level NPC (V_{a0}) for different overmodulation methods: (a) Minimum-Distance Error (90°); (b) Switching-State (60°); (c) Single-mode; (d) Dual-mode.

2) harmonic distortion, and 3) number of commutations. A finding is that by decreasing the angle between the voltage vector added to the original voltage command and the hexagon boundary, linearity is increased at the price of an increase in the harmonic distortion and number of commutations. It is concluded that none of the analyzed methods achieve the best performance for the whole overmodulation range and switching to fundamental frequency ratio. Optimal performance would be achieved by combining Switching-State and the Dual-mode. Preliminary simulation and experimental results have been provided.

Analysis of the dynamic transition between different overmodulation methods, both for open loop operation as well as in current controlled drives is a subject of ongoing research.

REFERENCES

- [1] X. Guo, M. He, and Y. Yang, "Over modulation strategy of power converters: A review," *IEEE Access*, vol. 6, pp. 69 528–69 544, 2018.
- [2] H. Mahlfeld, T. Schuhmann, R. Döbler, and B. Cebulski, "Impact of overmodulation methods on inverter and machine losses in voltage-fed induction motor drives," in *2016 XXII International Conference on Electrical Machines (ICEM)*. IEEE, 2016, pp. 1064–1070.
- [3] S. Halasz, I. Varjasi, and A. Zacharov, "Overmodulation strategies of inverter-fed ac drives," in *Proceedings of the Power Conversion Conference-Osaka 2002 (Cat. No. 02TH8579)*, vol. 3. IEEE, 2002, pp. 1346–1351.
- [4] G. Narayanan and V. T. Ranganathan, "Extension of operation of space vector pwm strategies with low switching frequencies using different overmodulation algorithms," *IEEE Transactions on Power Electronics*, vol. 17, no. 5, pp. 788–798, 2002.
- [5] S. K. Mondal, B. K. Bose, V. Oleschuk, and J. O. P. Pinto, "Space vector pulse width modulation of three-level inverter extending operation into overmodulation region," *IEEE Transactions on Power Electronics*, vol. 18, no. 2, pp. 604–611, 2003.
- [6] A. K. Gupta and A. M. Khambadkone, "A general space vector pwm algorithm for multilevel inverters, including operation in overmodulation range," *IEEE Transactions on Power Electronics*, vol. 22, no. 2, pp. 517–526, 2007.
- [7] J. Prieto, F. Barrero, M. J. Durán, S. T. Marín, and M. A. Perales, "Svm procedure for n -phase vsi with low harmonic distortion in the overmodulation region," *IEEE Transactions on Industrial Electronics*, vol. 61, no. 1, pp. 92–97, 2013.
- [8] P. Stumpf and S. Halász, "Optimization of pwm for the overmodulation region of two-level inverters," *IEEE transactions on industry applications*, vol. 54, no. 4, pp. 3393–3404, 2018.
- [9] J. Chen, R. Ni, T. Li, R. Qiu, and Z. Liu, "The harmonic characteristic of the advanced synchronous svpwm overmodulation strategy," *IEEE Access*, vol. 7, pp. 148 934–148 949, 2019.
- [10] A. M. Hava, R. J. Kerkman, and T. A. Lipo, "Carrier-based pwm-vsi overmodulation strategies: analysis, comparison, and design," *IEEE Transactions on Power Electronics*, vol. 13, no. 4, pp. 674–689, 1998.
- [11] S. Bolognani and M. Zigliotto, "Novel digital continuous control of svm inverters in the overmodulation range," *IEEE Transactions on Industry Applications*, vol. 33, no. 2, pp. 525–530, 1997.
- [12] J. Holtz, W. Lotzkat, and A. M. Khambadkone, "On continuous control of pwm inverters in the overmodulation range including the six-step mode," *IEEE Transactions on Power Electronics*, vol. 8, no. 4, pp. 546–553, 1993.
- [13] Dong-Choon Lee and G-Myoung Lee, "A novel overmodulation technique for space-vector pwm inverters," *IEEE Transactions on Power Electronics*, vol. 13, no. 6, pp. 1144–1151, 1998.
- [14] A. M. Hava, S.-K. Sul, R. J. Kerkman, and T. A. Lipo, "Dynamic overmodulation characteristics of triangle intersection pwm methods," *IEEE Transactions on Industry Applications*, vol. 35, no. 4, pp. 896–907, 1999.
- [15] Y.-C. Kwon, S. Kim, and S.-K. Sul, "Six-step operation of pmsm with instantaneous current control," *IEEE Transactions on Industry Applications*, vol. 50, no. 4, pp. 2614–2625, 2014.